Journal of Applied Polymer Science

Nonlinear Optical Materials by Electrospinning Technique

Fabio De Matteis,[1,2] Francesco Fanicchia,[3] Francesca Romana Lamastra,[2] Glauco Stracci,[1,3*] Roberta De Angelis,[3] Paolo Prosposito,[1,2] Francesca Nanni,[1,2] Mauro Casalboni[1,2]

[1]Department of Industrial Engineering, University of Rome Tor Vergata, Rome 00133, Italy

[2]Italian Interuniversity Consortium on Materials Science and Technology (INSTM), Research Unit Roma Tor Vergata, Rome 00133, Italy

[3]Department of Physics, University of Rome Tor Vergata, Rome 00133, Italy

*Present address: ENEA, Italian National Agency for New Technologies, Energy and Sustainable Economic Development, Via Anguillarese 301, Rome 00123, Italy

Correspondence to: F. De Matteis (E-mail: dematteis@roma2.infn.it)

ABSTRACT: The possibility of using electrospinning to deposit, and simultaneously electrically pole, polymeric mats containing nonlinear optical (NLO) molecules is studied. Disperse Red 1 (DR1) chromophore dispersed into polymethyl methacrylate (PMMA) fibers is chosen as test system. Aligned fibers of DR1/PMMA are deposited by means of the rotating collector electrospinning technique. The processing parameters are optimized to obtain an oriented texture of fibers and the NLO activity is characterized by means of second harmonic generation measurements. Comparison with spin coating and corona poling samples of the same material is discussed. The results point toward a low efficiency of chromophore orientation for the electrospun samples in comparison to the poled ones. An improvement in the electrospinning apparatus is proposed to enhance the chromophore orientation in the polymeric fibers. © 2014 Wiley Periodicals, Inc. J. Appl. Polym. Sci. **2014**, *131*, 40913.

KEYWORDS: electrospinning; fibers; optical and photovoltaic applications

Received 7 March 2014; accepted 23 April 2014
DOI: 10.1002/app.40913

INTRODUCTION

Polymer-based electrooptical (EO) materials represent a valid alternative to conventional inorganic crystalline materials, such as $LiNbO_3$ or KH_2PO_4, for applications in nonlinear optical (NLO) devices.[1–3] There are two specific features of polymeric materials which have boost a lot of efforts in the research in this field. The first is low spectral dispersion in the refractive index, in a wide region of the electromagnetic spectrum, allowing for travelling wave infrared modulators to operate at very high modulation frequency (>100 GHz) with relatively long interaction lengths (1 cm).[4] The second is the possibility to achieve robust and low-cost optoelectronic devices by monolithical integration of EO polymer devices on semiconductor electronics.[5] The electrical and optical properties of organic materials can be tailored by organic synthesis yielding, for instance, large EO coefficients and low drive voltages by the incorporation of molecules (chromophores) with large NLO properties.[6–9] The price to be paid is the need to undergo a poling process to destroy the centrosymmetric nature which is intrinsic in such amorphous materials. A macroscopic order is typically achieved in polymeric NLO materials by the application of an external electric poling field, which induces the alignment of the molecular electric dipole moments of intrinsically axial chromophores.[10] Postdeposition electric field orientation can be performed using different geometries, as in the case of corona poling,[11] parallel-plate, and coplanar-electrode poling.[12] In all these cases, high values of electric field are applied (up to 10^6 V/m).

In this study, we study the possibility of using the electrospinning technique to deposit, and simultaneously electrically pole, polymer fibrous mats containing NLO-active molecules. Electrospinning is a deposition technique first adopted in the early 1900, which has seen a flourishing of interest at the half of 1990s with the explosion of the nanotechnologies.[13,14]

In addition, it is an effective method to disperse nanofillers (i.e., carbon nanotubes, graphene nanoplatelets, and ceramic nanoparticles) into a polymer fiber matrix.[15,16] In this study, we aim to explore the possibility of using the same electric field which drives the extrusion of the polymeric fibers, to orient the NLO molecules along a preferential direction in the polymeric fiber matrix during the deposition. The advantage of this technique for NLO fiber formation would be related to the possibility to simultaneously deposit and electrically pole a NLO material.

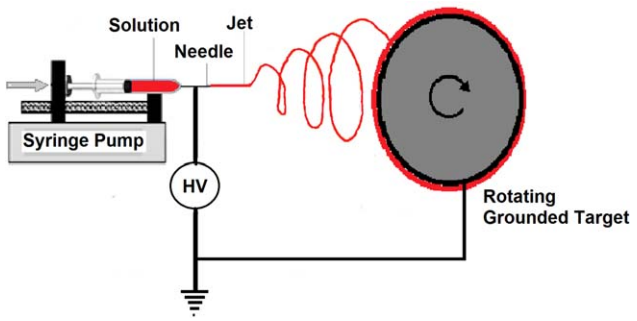

Figure 1. Scheme of electrospinning apparatus. [Color figure can be viewed in the online issue, which is available at wileyonlinelibrary.com.]

The test system chosen in this study is Disperse Red 1 (DR1) chromophore dispersed into polymethyl methacrylate (PMMA). Well-aligned DR1/PMMA fibers have been obtained by means of the rotating collector electrospinning technique. The deposition parameters have been carefully optimized to obtain an oriented texture of fibers and the NLO activity has been characterized by means of second harmonic generation (SHG) measurements.

EXPERIMENTAL

PMMA solutions (10 and 14% wt %) were prepared by dissolving the polymeric powder (PMMA, MW = 350,000, Aldrich) in dimethylformamide (DMF) under stirring for 24 h. Commercial chromophore DR1 (Sigma-Aldrich) was added at 10% wt % with respect to PMMA. The resulting mixtures were sonicated for 1 h and then poured in a glass syringe (Hamilton, Carlo Erba) equipped with a 20 G needle, fixed in a digitally controlled syringe pump (KD Scientific, MA, USA). The needle was connected to a high-voltage supply (Spellman, Model SL 30, NY, USA) able to generate DC voltages up to 30 kV.

Grounded aluminum cylinders of different diameters, either static or rotating at 2700 rpm, were used to collect electrospun fibers. The processing parameters adopted were as follows: voltage, 12 kV; needle-target distance, 15 cm; and flow rate, 1 or 0.5 mL/h.

Neat PMMA solutions were also electrospun for comparison. The scheme of electrospinning apparatus is shown in Figure 1 and Table I summarizes all the electrospun samples.

Morphology of electrospun mats was examined by field emission scanning electron microscopy (FEG-SEM, Leo Supra 35) on gold-sputtered samples.

SHG experimental set-up, described in detail elsewhere,[17] consists of a Quantel Brilliant Q-switched Nd:YAG laser (repetition frequency, 10 Hz; pulse duration, 5 ns; 400 mJ per pulse) which provides the fundamental beam output at 1064 nm for the measurements of SHG. This source feeds a Solid-State Raman Shifter (MolTech CRS-14, Barium Nitrate) which shifts the beam output to 1368 nm to avoid resonance enhancement of the NLO signal. The Corona poling was performed by means of a high-voltage generator grounded to the heating stage and the whole apparatus was held in a controlled atmosphere (dry-nitrogen) box. The poling voltage and time was optimized to fully preserve chemical integrity of the materials. The final value for applied voltage and poling time were 8 kV and 13 min, respectively. The typical poling procedure consisted of heating the sample at 90°C (a temperature below the glass transition temperature of the polymer), with the electric field on. The film was then cooled down to room temperature at 1°C/min and the electric field was finally switched off at room temperature.

RESULTS AND DISCUSSION

Morphology of Electrospun Mats

We report the list of samples used in the study with the respective deposition parameters listed in Table I. Scanning electron microscopy (SEM) micrographs of all electrospun samples are shown in Figures 2 and 3.

As expected, samples collected on static targets (PA4 and DR1A) are random fiber mats with a mean diameter of 0.7 and 0.5 μm, respectively [Figure 2(a,b)]. The slightly lower fiber size observed for DR1A could be associated to the lower flow rate adopted in electrospinning.

SEM observations on PA7RC and DR1-1, deposited on rotating cylinder with ø 1.6 cm, show partially aligned fibers and in the case of the former sample bead formation [Figure 2 (c,d)]. In addition, it was revealed again that a lower flow rate leads to a smaller fiber average diameter.

SEM micrographs of PA8R, DR1-2, and DR1-4 display that an increase of the diameter of the collecting target results in an improvement of the degree of alignment of fibers [Figure 3 (a–f)]. In addition, the increase of polymer concentration from

Table I. Electrospun Samples

	Starting solution				
Sample (units)	PMMA (wt %)	DR1	Flow rate (mL/h)	Target	Mean diameter (μm)
PA4	10	No	1	Static cylinder ø 6 cm	0.7
DR1-A	10	Yes	0.5	Static cylinder ø 6 cm	0.5
PA7R-C	10	No	0.5	Rotating cylinder ø 1.5 cm	0.38
DR1-1	10	Yes	1	Rotating cylinder ø 1.5 cm	0.5
DR1-2	10	Yes	0.5	Rotating cylinder ø 6 cm	0.3
PA8R	14	No	0.5	Rotating cylinder ø 6 cm	1.0
DR1-4	14	Yes	0.5	Rotating cylinder ø 6 cm	1.1

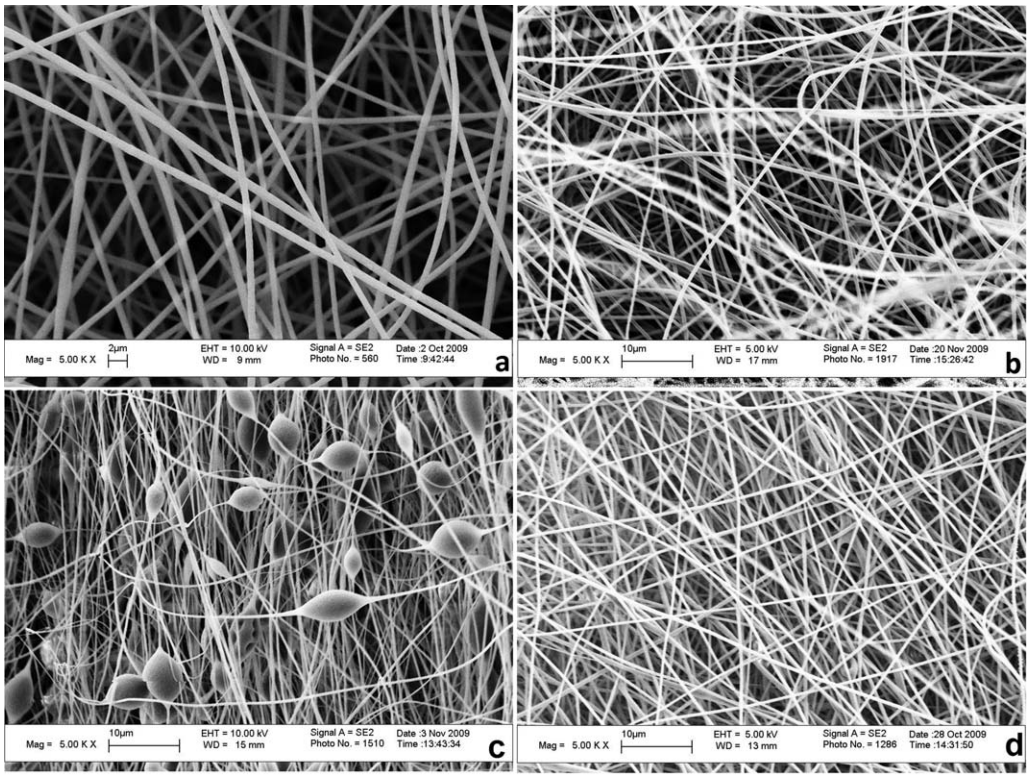

Figure 2. SEM micrographs of (a) PA4, (b) DR1A, (c) PA7RC, and (d) DR1-1.

10 to 14% wt % increases remarkably the average fiber diameter and prevents bead formation. The addition of DR1 does not seem to have a significant influence on fiber size being the mean diameter 1.0 and 1.1 μm for PA8R and DR1-4 samples, respectively. A comparison between DR1A and DR1-2 micrographs reveals that the collecting target also affects the morphology. Particularly, the use of the rotating target with respect to the static one leads to some beaded fibers and to a smaller mean fiber diameter.

Fast Fourier Transform Analysis

The Fast Fourier Transform (FFT) has been used to characterize the fiber alignment as a function of spinning experimental parameters. FFT generates an image which is a graphical representation of the frequency content of the starting image. The SEM micrographs obtained from the samples have been processed by a FFT routine of the image processing software ImageJ (NIH). The pixel intensity of the resulting FFT image gives an indication of the fiber orientation in the real space. The sum of the pixel intensities along a line (at a fixed angle θ) from the center to the border of the image yield the relative contribution of the objects oriented along that direction.

The FFT analysis of three different samples is shown in Figure 4. Figure 4(a) refers to sample DR1-A which was deposited on a static cylinder, whereas Figure 4(b,c) refer, respectively, to samples DR1-1 and DR1-4 which were deposited using a rotating cylinder. The comparison between the three samples shows that the rotation of the target cylinder produces the alignment of the electrospun fibers. Larger cylinders produce better alignment.

SHG Measurements

The NLO activity of DR1-4, the sample which showed the better alignment of the fibers, has been studied by means of the measurements of SHG. The sheet of fibers, as obtained by the electrospinning apparatus, does not show a sufficient optical transparency owing to the intrinsic inhomogeneity of the textured material as shown in Figure 5(a). Therefore, we have pressed the sheet by means of a hydraulic press (100 bar for 90 s). The sample was sandwiched between two BK7 slides to easily manipulate the sample.

The same DMF solution of the polymer with 10% wt % of DR1 (sample DR1-4) was used for spin-coating deposition. A thin film of PMMA doped with DR1 was spin coated on BK7 glass substrate at 4000 rpm for 40 s to obtain homogenous film with a thickness of the order of 1 μm. The spin-coated film was treated by corona poling to break the centrosymmetry of the chromophore alignment. The absorption spectra of the electrospun DR1-4 sample and the spin-coated film are compared in Figure 6. A saturation of the absorption is evident for the DR1-4 sample as a consequence of the thickness of that sample (28 μm), whereas the spin-coated PMMA-DR1 film was 2 μm. Although the saturation of the absorption does not allow to study the details of the linear optical behavior (e.g., light-polarization dependence), the overall transparency of the electrospun sample suggests the possibility of performing the measurements of NLO in the NIR–VIS spectral region.

The SHG signal from the DR1-4 sample was compared with that obtained, at the same conditions, on the PMMA-DR1 spin-coated film. The direction of preferential molecular alignment is

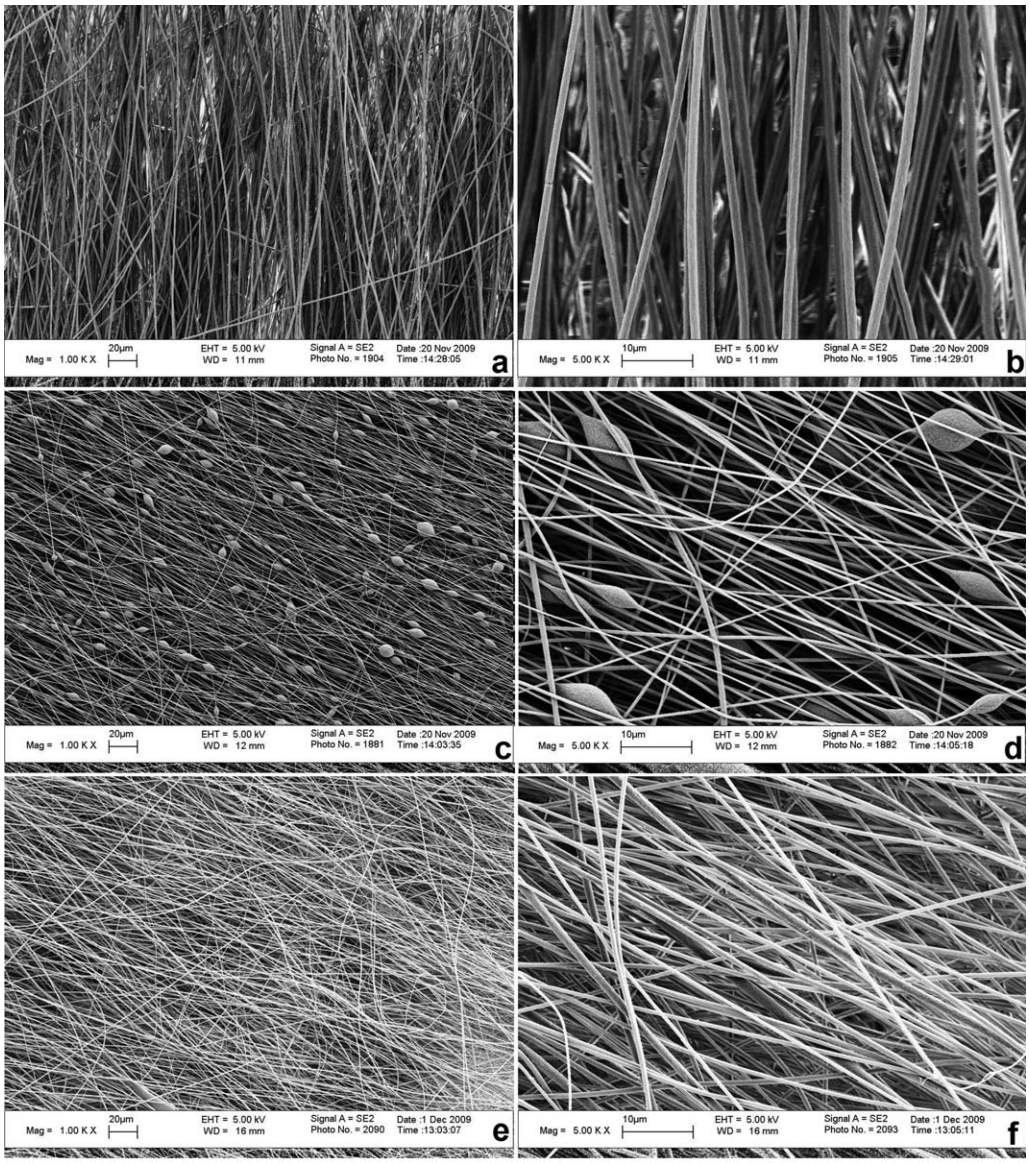

Figure 3. SEM micrographs of (a,b) PA8R, (c,d) DR1-2, and (e,f) DR1-4.

perpendicular to the film for corona-poled samples. Therefore, it is necessary to launch the fundamental light beam at a nonzero incidence angle. The SHG signal was measured at an incidence angle of 20° for both samples and normalized to the reference value measured on a crystalline quartz slide on a secondary arm of the optical setup. The relative error on the SHG measurement was estimated at 10% corresponding to the fluctuation of the signal.

The electrospun sample DR1-4 was measured with two mutually orthogonal orientation of the prevalent alignment direction of the fibers in the plane: parallel and perpendicular to the direction of incident light polarization. As the incident light was *p*-polarized, it was sufficient to measure at the two orthogonal directions to get an indication on the chromophore alignment in the fibers.

Parallel orientation gave SHG signal of 0.272 (arb.units), whereas perpendicular orientation produced a signal of 0.127 (arb.units). The NLO intensity was normalized with reference to the SHG intensity from a crystalline quartz slide.

Such a result is a clear indication of an effective optical anisotropy of the polymeric matrix caused by the preferential orientation of the chromophores along the fiber direction (preferential direction in the plane of the film). As expected, a clear reduction (>50%) of the SHG signal was observed by rotating the sample orientation from parallel to perpendicular to the plan of incidence of the light. Poled materials show a polar spatial symmetry ($C_{\infty v}$ symmetry system) for which only five components of the nonlinear susceptibility tensor are nonzero ($\chi^{(2)}_{333}$, $\chi^{(2)}_{311}=\chi^{(2)}_{322}$, $\chi^{(2)}_{113}=\chi^{(2)}_{223}$). It is often assumed $\chi^{(2)}_{311}/\chi^{(2)}_{333}=1/3$ and, within the Kleinman symmetry condition, $\chi^{(2)}_{113}=\chi^{(2)}_{311}$.[18]

From the values of the SHG signal of the sample with fibers oriented parallel and perpendicular to the plane of incidence,

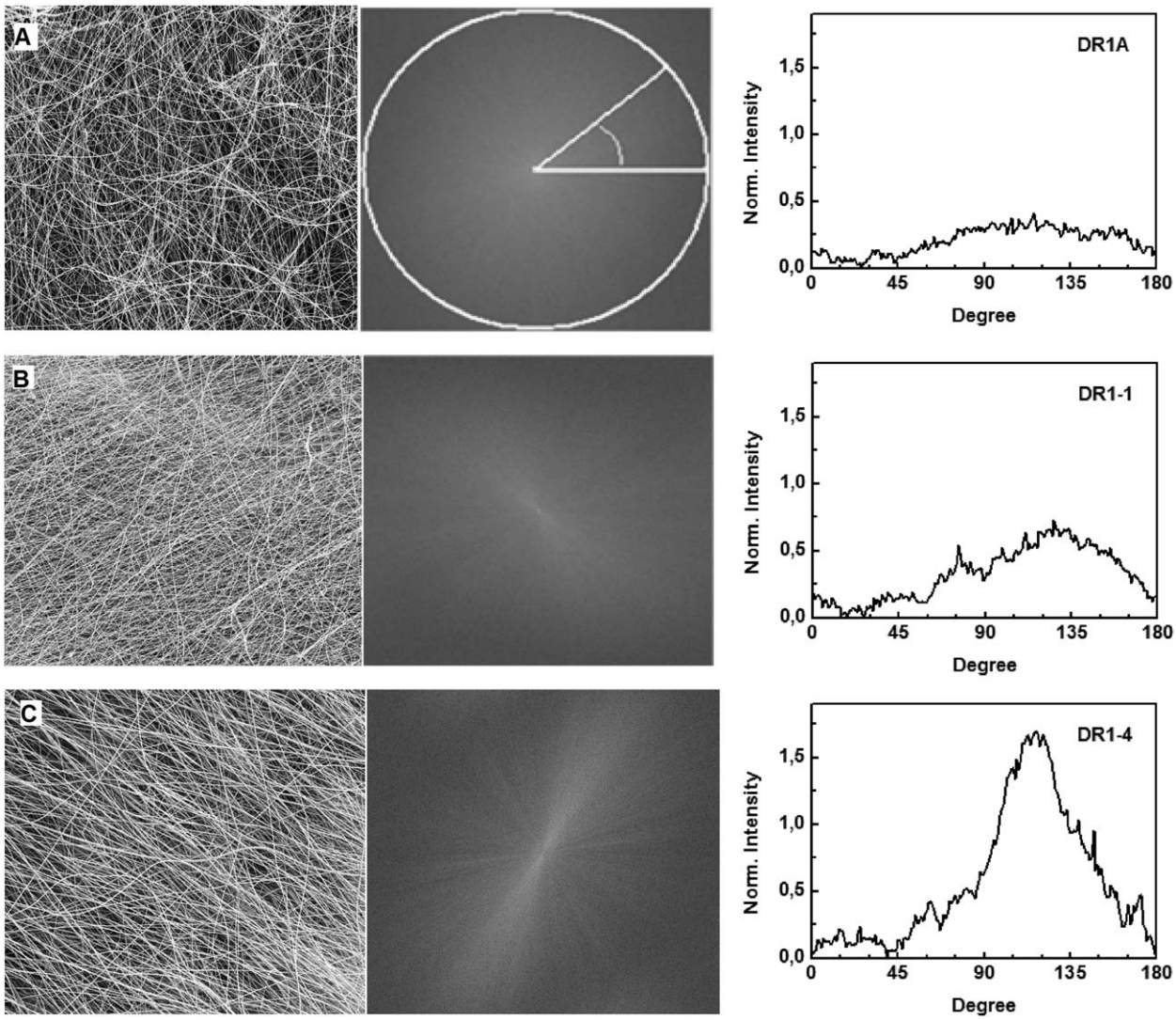

Figure 4. SEM micrographs of a random (a) partially, (a) best aligned, and (C) textures; the respective FFT images and angle–intensity graphs which describe the orientation distribution are shown.

the ratio of the two nonlinear coefficients is conjectured to be 1/4, not far from the usual assumed value. Deviations from 1/3 value for the ratio are frequently reported and are mostly related to differences in the poling procedure.[11]

On the other hand, the chromophores tend to be aligned perpendicularly to the film plane in the corona-poled samples. Therefore, the NLO properties are invariant for rotations in the plane of the film and a single SHG measurement has been recorded for those samples. The NLO intensity recorded for the poled film with the reference to the intensity from a crystalline quartz slide was 220 (arb.units).

The SHG signal differs by three orders of magnitude between poled and electrospun samples. The thickness as measured by mechanical profilometer was, respectively, 2 μm for the former and 28 μm for the latter. As the chromophore density in the starting PMMA solution was the same in the two cases, the SHG signal of the electrospun sample could be expected to be larger than that of the spin-coated one. The phase-matching condition should be considered as it could affect the coherent propagation length of the SHG wave for thick samples. The coherence length depends on the difference of the value of refractive index at the fundamental and second-order frequency. For polymers, out of resonance condition, such parameters are in the range of some microns: $l_c = \pi/\Delta k = \lambda/4|n_\omega \cos j_\omega - n_{2\omega} \cos j_{2\omega}|$.[11] At 1368 nm, a difference of 0.01 in the refractive index gives $l_c = 34$ μm. Therefore, in a first qualitative approach, the effect of phase matching was not taken into account.

The results point toward a low efficiency of chromophore orientation for the electrospun samples in comparison to the poled ones. In Figure 7, a graphical simulation of the electric field intensity shows how the region of high electric field is limited to a narrow region around the needle. Such a narrow region is not sufficient to yield a permanent alignment of the dipolar

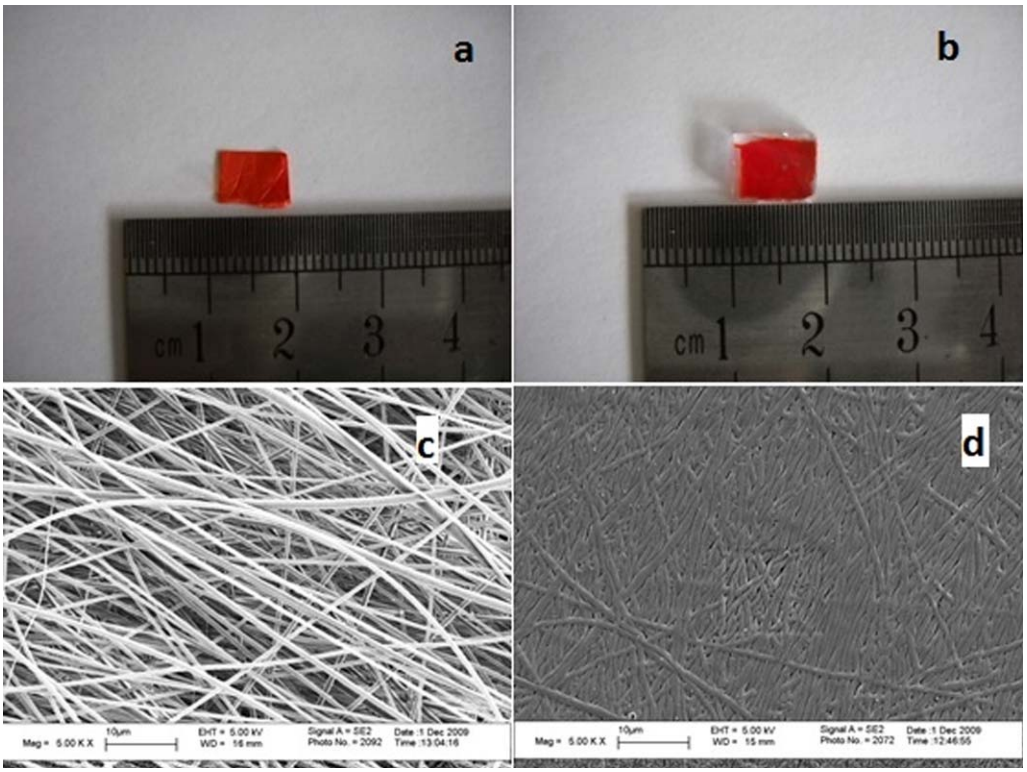

Figure 5. DR1-4 sample image and SEM micrographs before (a, c) and after (b,d) the pressing process on BK7 substrate. [Color figure can be viewed in the online issue, which is available at wileyonlinelibrary.com.]

molecules. When the wire exits the high electric field region, the polymer is still fluid enough to let occur a thermal reorientation of the polar molecules within the wire.

In spite of the negative result, still interesting perspectives can open if one manages to modify the shape of the electric potential around the needle to maintain a sufficiently strong electric field for a longer path. For instance, this could be obtained with one (or more) properly positioned ring electrode at an intermediate potential. The effect of the insertion of two metallic rings at intermediate potential values is shown in Figure 8.

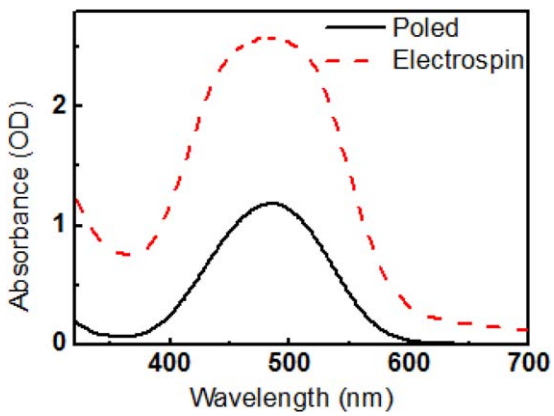

Figure 6. Absorption spectra of poled and electrospun samples after the press treatment. [Color figure can be viewed in the online issue, which is available at wileyonlinelibrary.com.]

A region of almost constant field is generated in the first part of the path where the electrospun wire moves. The first electrode sustains the potential drop (6 kV) with respect to the needle which determines the wire extrusion; the second ring produces a region of approximately constant electric field over a distance of some centimeters where the poling of the materials can occur; the rest of the path falls in a region of much lower

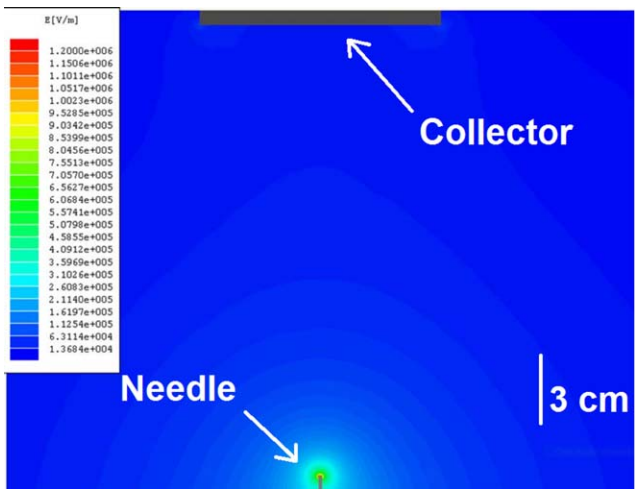

Figure 7. Simulation of the electric field intensity in the electrospin apparatus. The color gradient scale covers two orders of magnitude of the electric field intensity. [Color figure can be viewed in the online issue, which is available at wileyonlinelibrary.com.]

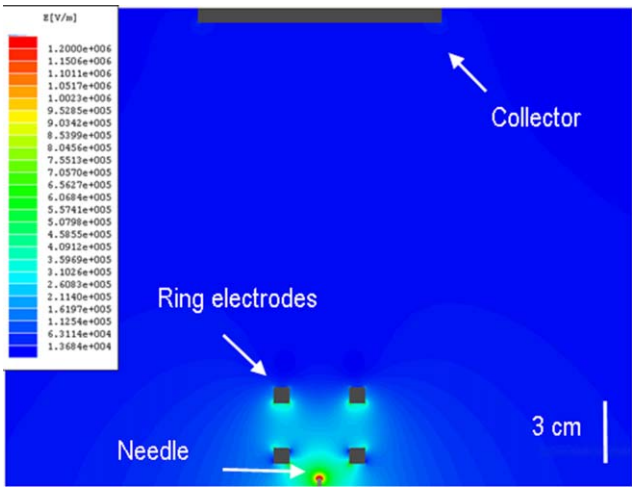

Figure 8. Simulation of the electric field intensity in the electrospin apparatus. The color gradient scale covers two orders of magnitude of the electric field intensity. [Color figure can be viewed in the online issue, which is available at wileyonlinelibrary.com.]

field where the wire moves almost inertially toward the collector. We are planning to improve our setup to test such hypothesis.

CONCLUSIONS

Aligned PMMA fibrous mats containing Disperse Red 1 as NLO-active molecules have been obtained and simultaneously electrically poled by means of electrospinning technique.

The processing parameters have been optimized to obtain fibers oriented along a preferential direction. Spin coating and corona poling samples of the same materials have been deposited for comparison. The measurements of SHG have shown that NLO activity is significantly lower for the electrospun samples in comparison to the spin-coated ones. This points toward a low efficiency of chromophore orientation which can be improved with a careful design of the electrospinning apparatus to enhance the chromophore orientation degree in the polymeric fibers.

ACKNOWLEDGMENTS

The financial support by Italian CARIPLO foundation through the project number 2010-0525 is gratefully acknowledged.

REFERENCES

1. Jang, S.-H.; Jen, A. K.-Y. In Introduction to Organic Electronic and Optoelectronic Materials and Devices; Sun, S.-S.; Dalton, L. R., Eds.; CRC Press: Boca Raton, **2008**; p 467.
2. Enami, Y.; Derose, C. T.; Mathine, D.; Loychik, C.; Greenlee, C.; Norwood, R. A.; Kim, T. D.; Luo, J.; Tian, Y.; Jen, A. K. Y.; Peyghambarian, N. *Nat. Photon.* **2007**, *1*, 180.
3. Prosposito, P.; De Matteis, F. In Advances in Macromolecules, Perspectives and Applications; Russo, M. V., Ed.; Springer: Berlin, **2010**; Chapter *2*, p 119.
4. Lee, M.; Katz, H. E.; Erben, C.; Gill, D. M.; Gopalan, P.; Heber, J. D.; McGee, D. J. *Science* **2002**, *298*, 1401.
5. Dalton, L.; Harper, A.; Ren, A.; Wang, F.; Todorova, G.; Chen, J.; Zhang, C.; Lee, M. *Ind. Eng. Chem. Res.* **1999**, *38*, 8.
6. Yang, J. X.; Wang, C. X.; Li, L.; Hao, F. Y.; Zhang, Q.; Tu, Y. L.; Wu, J. Y.; Xue, Z. M.; Tian, Y. P. *Chem. Phys.* **2009**, *358*, 39.
7. Ma, X.; Ma, F.; Zhao, Z.; Song, N.; Zhang, J. *J. Mater. Chem.* **2010**, *20*, 2369.
8. Borbone, F.; Carella, A.; Roviello, A.; Casalboni, M.; De Matteis, F.; Stracci, G.; Della Rovere, F.; Evangelisti, A.; Dispenza, M. *J. Phys. Chem. B* **2011**, *115*, 11993.
9. Centore, R.; Riccio, P.; Fusco, S.; Carella, A.; Quatela, A.; Schutzmann, S.; Stella, F.; De Matteis, F. *J. Polym. Sci. Polym. Chem.* **2007**, *45*, 2719.
10. De Matteis, F. *Ferroelectrics* **2007**, *352*, 11.
11. Burland, M.; Miller, R. D.; Walsh, C. A. *Chem. Rev.* **1994**, *94*, 31.
12. Palazzesi, C.; Stella, F.; De Matteis, F.; Casalboni, M. *J. Appl. Phys.* **2010**, *107*, 113101.
13. Doshi, J.; Reneker, D. H. *J. Electrostat.* **1995**, *35*, 151.
14. Teo, W. E.; Ramakrishna, S. *Nanotechnology* **2006**, *17*, R89.
15. Lamastra, F. R.; Puglia, D.; Monti, M.; Vella, A.; Peponi, L.; Kenny, J. M.; Nanni, F. *Chem. Eng. J.* **2012**, *195–196*, 140.
16. Nanni, F.; Lamastra, F. R.; Pisa, F.; Gusmano, G. *J. Mater. Sci.* **2011**, *46*, 6124.
17. Franco, A.; Brusatin, G.; Guglielmi, M.; Stracci, G.; De Matteis, F.; Casalboni, M.; Detert, H.; Grimm, B.; Schrader, S. *J. Non-Cryst. Solids* **2010**, *356*, 1689.
18. Boyd, R. W. In Nonlinear Optics, 2nd ed.; Academic Press: London, **2003**.